Combining hydrogeochemistry, statistics and explorative mapping to estimate regional threshold values of trace elements in groundwater (Sardinia, Italy)

Elisabetta Dore[a], Riccardo Biddau[a], Mario Lorrai[b], Paolo Botti[b], Antonella Buccianti[c], Franco Frau[a], Rosa Cidu[a*]

[a] Department of Chemical and Geological Sciences, University of Cagliari, Blocco A Monserrato, Italy

[b] Regione Autonoma della Sardegna-ADIS-Servizio tutela e gestione delle risorse idriche, via Mameli 88, 09100 Cagliari, Italy

[c] Department of Earth Sciences, University of Florence, Florence, Italy

[*] Corresponding Author *e*-mail: cidur@unica.it

Abstract

Assessing baseline and threshold values of potentially toxic elements at adequate scales is fundamental for distinguishing geogenic contamination from anthropogenic pollution in groundwater. This study was aimed to estimate the regional threshold values of Li, Be, B, Al, V, Cr, Mn, Fe, Co, Ni, Cu, Zn, As, Se, Rb, Sr, Mo, Ag, Cd, Sb, Te, Ba, Hg, Tl, Pb, Bi, U in groundwater, compare results to guidelines established for drinking water and the protection of groundwater from contamination, investigate the geographical distribution of trace elements, and assess the potential influence of rocks with which groundwater interacts.

A pre-selection aimed at excluding groundwater samples affected by known anthropogenic activities was carefully carried out based on hydrogeochemical characteristics of waters and considering the potential sources of contamination. The resulting dataset was comprised of 1239 groundwater sampling sites located in Sardinia (Italy). Undetected values were treated using the Regression on Order Statistics method. For elements containing more than 75 % of undetected values and/or a limited number of samples in the dataset (Li, Rb, Sr, Mo, Ag, Te, Tl, Sb, Hg and Bi), the threshold values were estimated using either the 95th or 97.7th percentiles. For the other elements the mean+2SD (Standard Deviation), the median+2MAD (Median Absolute Deviation), and the TIF (Tukey Inner Fence) estimators were also calculated.

In general, the 95th threshold value of the trace element in groundwater was adequate when referring to the regional scale, whereas other estimators might be more appropriate at the local scale. Regional threshold values of the regulated elements B, Al, V, Cr, Cu and Cd in groundwater were below the Italian and World Health Organization drinking water guidelines, whereas Mn and As were above them. Regional threshold values estimated with TIF exceeded the drinking water guidelines for Ni, Se, Pb and U.

Maps of As, Sb, Cd, Pb and U showed concentrations above regional threshold values mainly corresponding with groundwater interacting with geological complexes hosting known mineral deposits, either mined or unexploited.

Results of this study showed that high concentrations of trace elements in groundwater were primarily dependent on the corresponding amount in parent materials with which the groundwater came into contact. Physical-chemical parameters and geochemical characteristics may contribute to enhancing concentrations of some trace elements in groundwater, e.g. As via reductive dissolution of Fe(III)-Mn(IV) hydroxides/oxides, Pb via formation of stable aqueous complexes, and other elements via adsorption onto fine particles with size below 0.4 µm (i.e. the pore size of filters used). Maps drawn on the centered log-ratio (*clr*) transformation of hydrogeochemical data, following the CoDA (Compositional Data Analysis) approach, gave additional information useful to pinpoint critical areas to be investigated in more detail. For each geological complex, groundwater samples likely representing nearly pristine conditions were identified. The monitoring of these representative groundwater samples may help to pinpoint eventual changes in environmental conditions.

Keywords

groundwater, trace elements, threshold values, mapping, compositional data analysis (CoDA), Sardinia,

1. Introduction

Trace elements naturally occurring at parts per million levels in the Upper Continental Crust (Rudnick and Gao, 2014) are generally present at parts/sub-parts per billion concentrations in natural waters. The occurrence of trace elements in groundwater can be due either to natural sources, such as dissolution of minerals that come into contact with the water, or human activities, such as mining, fuel use, ore smelting and improper disposal of industrial and urban wastes (Appelo and Postma, 1993). Trace elements such as Mn, Fe, Co, Ni, Cu and Zn are essential micronutrients for biota within a defined range of concentrations (Lohan and Tagliabue, 2018). However, other elements such as Cr, As, Cd, Sb, Hg and Pb are known to be toxic to biota and high concentrations in groundwater may pose a threat to human health, as recognized by the World Health Organization (WHO, 2017). So, health-based targets should be established for the drinking water, as a part of overall water and health policy (WHO, 2017).

In some cases, several toxic or harmful elements may occur in groundwater at high geogenic (natural) concentrations. It is the case of groundwater interacting with unexploited ore deposits and/or specific rock types, such as serpentinite (Binda et al., 2018), black shale (Parviainen and Loukola-Ruskeeniemi, 2019), and ultramafic rocks (Sahoo et al., 2019; Kierczak et al., 2021) that may be enriched in Ni, V, Cr, Cu, Zn and Mn. Therefore, it is essential to determine the geochemical baseline level (i.e. the actual background) of trace elements in groundwater with the aim to distinguish high concentrations due to natural sources (i.e., geogenic and biological processes) from contamination due to anthropogenic activities, such as urbanization, industrial activities, mining and agricultural practices. The threshold value (i.e. the upper limit of the natural background) is commonly used as a practical reference value to evaluate the *good* status of groundwater quality (Langmuir, 1997; Edmunds et al., 2003).

The best method of defining the geochemical background and the related threshold value is a matter of much discussion, and several approaches have been proposed (e.g.: Matschullat et al., 2000; Reimann et al., 2005; ISPRA, 2018; Reimann et al., 2018; Parrone et al., 2019; Zanotti et al., 2022). Methods include the calculation of percentiles of a given dataset (e.g.: 90^{th}, 95^{th} and 97.7^{th} percentile); the Median±2 Median Absolute Deviations (MAD), the study of inflection points in a cumulative probability plot and the Tukey Inner Fence (TIF) estimator calculated as follows: 75^{th} percentile + 1.5 IQR, where IQR is the interquartile range (75^{th} - 25^{th} percentile). Because distributions of geochemical data are most often strongly right-skewed, in order to achieve a symmetrical (but not necessarily normal) data distribution, the correct approach would be to perform calculations on the logarithmic transformed data (Allegre and Lewin, 1995; Reimann et al., 2018; Gozzi et al., 2020). Moreover, the compositional nature of geochemical data is also to be taken into account and should be considered in statistical analysis of geochemical data (Buccianti and Grunsky, 2014; Boente et al., 2022).

The concentrations of substances dissolved in groundwater may vary considerably in space and time. A high variability in the chemistry of groundwater may occur locally, particularly in geological environments in which marked variations in lithology occur both laterally and at depth. These conditions pose difficulties in establishing the geochemical background at a variety of scales. It is not possible to recognize and understand changes in natural systems if the natural background range has never been documented and mapped (Zoback, 2001). Geochemical maps at the continental-scale have been published in the United States (Smith et al., 2014) and Europe (Reimann et al., 2014a, 2014b). These datasets have been used to establish the geochemical background variation at the continental scale and, in Europe, for risk assessment of metals in the environment (e.g., Oorts and Schoeters, 2014; Birke et al., 2016).

In summary, for assessing the impact of contaminants on groundwater systems, and eventually establishing regulatory limits, and groundwater remediation programs, it is mandatory to know the baseline concentrations of contaminants at an adequate scale. This study was based on data acquired by hydrogeochemical investigations carried out in Sardinia (Italy). In this region, many areas are unaffected by diffuse anthropogenic pollution that allow to evaluate the present status of groundwater quality, possibly close to nearly pristine conditions. However, Sardinia hosts widespread mineralization, both mined and not exploited, which makes challenge the baseline evaluation of trace elements.

Specific objectives of this study were to: *i)* assess the regional occurrence of trace elements Li, Be, B, Al, V, Cr, Mn, Fe, Co, Ni, Cu, Zn, As, Se, Rb, Sr, Mo, Ag, Cd, Sb, Te, Ba, Hg, Tl, Pb, Bi, U (elements listed according to atomic numbers) in Sardinian groundwater; *ii)* calculate the regional threshold values of trace elements using different estimators and compare results with guidelines established for drinking water and the protection of groundwater; *iii)* draw explorative maps for investigating the geographical distribution of trace elements, also considering the compositional data analysis (CoDA) approach; *iv)* assess the potential influence of rock composition on concentrations of trace elements in groundwater.

2. Study area

The study area is located in Sardinia (Italy), an island extending 24,090 km^2 in the western Mediterranean Sea. Sardinia hosts 1,672,000 inhabitants mainly located in few cities (ISTAT, 2011). The average altitude is 334 m above sea level (asl). Mountains (19% of land) with maximum elevation of 1834 m asl are mainly located in the eastern part. Hills (68% of land) prevail over flat areas, such as the Campidano Plain and the river mouths. Forests (53% of land), pastures and forages (43% of land) represent semi-natural and poorly-developed rural areas. Industries are mainly located nearby the cost (Fig. 1), with limited influence on water bodies inland.

Climatic conditions in Sardinia vary from semi-arid in the plain to semi-humid in the mountains. Mean temperatures range from 5 °C in winter to 25 °C in summer. The mean precipitation is in the range of 500 to 1100 mm per year, with about 50 to 90 rainy days per year; heavy-rain events have been increased in the last decades.

A simplified lithological map of Sardinia showing the location of relevant mines, mineralized areas (Marcello et al., 2008; De Vivo et al., 1998; Palomba et al., 2006), and industrial sites is shown in Figure 1. Sardinian geological records can be summarized as follows (Carmignani et al., 2015): (a) the Paleozoic basement, mostly extending in the eastern part of the island, that underwent repeated phases of deformation and metamorphism during the Caledonian and Hercynian orogenic cycles, and locally intruded by calc-alkaline granitic rocks; (b) the Mesozoic carbonate sequence that formed the passive margin of Southern Europe; (c) the calc-alkaline volcanic rocks (Tertiary), alkaline basalts (Quaternary), and sedimentary cover consisting of shallow-water marine carbonates, siliciclastic sediments and continental conglomerates (Tertiary to Quaternary).

Sardinia was a relevant mining region in Italy and Europe, with Zn-Pb(Ag)-Cu-Ba-Sb exploitation carried out intensively since 1880 till 1990. Stratabound deposits are the more economic ores in Sardinia. They are often hosted in the Lower Paleozoic rocks in southwest Sardinia (Iglesiente-Fluminese, Fig. 1) where sphalerite-galena-barite deposits may occur as massive sulfides and partly as Mississippi Valley type (De Vivo et al., 1998; Moroni et al, 2019). In central and southeast Sardinia, stratabound mineralization consists of scheelite, arsenopyrite, antimonite (Gerrei, Fig. 1), and chalcopyrite-sphalerite-galena massive sulfides (Funedda et al., 2018). Some skarn deposits are connected to the granite intrusion (Naitza et al., 2017). Auriferous mineralization associated with sulfide minerals was discovered in Tertiary volcanic rocks, and a gold mine was active at Furtei (Fig. 1) in central Sardinia from 1997 to 2003 (Cidu et al., 2013, and references therein). Post-Hercynian hydrothermal deposits with barite, fluorite, galena, antimonite and argentite were documented in the Tertenia area (Fig. 1., Lorrai and Mereu, 1999), bauxite in the Nurra (Mameli et al., 2007; Mongelli et al., 2021), and kaolin, bentonite and zeolite deposits in several parts of the island (Palomba et al., 2006; Mormone and Piochi, 2020).

Actually, the abandoned mines pose serious environmental hazards, particularly due to the weathering of mining-related wastes dumped nearby the mines, and the presence of highly contaminated groundwater flowing out of adits.

3. Methods

3.1 Data source

The dataset used in this study was derived from several hydrogeochemical surveys carried out at the University of Cagliari (UNICA, Biddau et al., 2017 and reference therein) and from the groundwater monitoring program established by the Sardinian Regional Government (RAS, 2011). Hydrogeochemical surveys at UNICA were focused either on mine areas for assessing the impact of mining on the water quality, or in nearly pristine areas for investigating water-rock interaction processes. Sampling density and measured chemical elements were dependent on specific objectives established in each survey, therefore, the distribution of groundwater samples in the region was not homogeneous. The RAS groundwater-monitoring program is a long-term activity aimed to identify temporal trends in groundwater quality at the regional scale. The RAS monitoring sites included fresh groundwater from relevant water bodies, groundwater in areas of environmental relevance (e.g. wetlands) and target areas at industrial sites. For this study, analyses derived from the RAS surveys carried out in winter and summer in 2016 were available. Results on physical-chemical parameters, major components, nitrogen species and fluoride were published elsewhere (Biddau et al., 2017, and reference therein).

As an attempt to assess the status of groundwater as close as possible to natural conditions, the whole dataset was carefully submitted to a pre-selection aimed at excluding any sample affected by known anthropogenic

inputs. Hydrogeochemical features of groundwater samples were carefully considered in the pre-selection. The Piper diagrams and binary plots comprising concentrations of major and trace components, together with concentrations of nitrogen species and phosphate, were useful for recognizing anthropogenic contamination. On the basis of pre-selection results, groundwater located at/downstream of industrial sites, in the nitrate vulnerable zone (NVZ) of Arborea (Fig. 1; RAS, 2005), in areas affected by past-mining activities, and in coastal areas affected by the intrusion of modern seawater due to over-exploitation were excluded. Thermal waters, waters collected at wells with unknown construction details, and waters showing calculated charge balance errors > 10 % were also excluded. The dataset resulting from the pre-selection included 1239 sampling sites. Physical-chemical parameters and major chemical components have been reported elsewhere (Biddau et al., 2017), thus are not discussed in this paper.

Depending on specific objectives to be achieved in each survey, Li, Rb, Sr, Mo, Te, Tl and Bi were only determined at 192 (Te) to 376 (Sr) groundwater sampling sites. Elements Be, B, Al, V, Cr, Mn, Fe, Co, Ni, Cu, Zn, As, Se, Ag, Cd, Sb, Ba, Hg, Pb, and U were determined at 984 (V) to 1227 (B) groundwater sampling sites. Location of sampling sites is shown in the geochemical maps that will be presented later.

On the basis of physical-chemical parameters and chemical components, a careful interpretation of the geochemical data, coupled with hydrogeological information, made it possible to identify 9 groups of samples according with the geological complex with which the groundwater comes into contact: Quaternary sediment, Quaternary basalt, Tertiary sediment, Tertiary andesite, Tertiary ignimbrite, Mesozoic carbonate, Paleozoic granite, Paleozoic metamorphic, and Paleozoic carbonate.

3.2 Analytical protocols and data quality

The analytical protocol for trace elements can be summarized as follows. On site, the water was filtered (0.4 μm pore size) into pre-cleaned, high-density polyethylene bottles, acidified immediately upon filtration to 1% (v/v) HNO_3 supra pure, and stored refrigerated until analyses. Chemical analyses in the RAS groundwater-monitoring program were carried out at certified laboratories (RAS, 2011).

In surveys carried out at UNICA, elements B, Fe, Mn, Co, Cu, Zn, Sr, Cd and Ba were determined both by inductively coupled plasma optical emission spectrometry (ICP-OES, ARL 3520) and ICP mass spectrometry (ICP-MS, PerkinElmer ELAN5000 and ELAN DRC-e). Elements Be, Al, V, Cr, Co, Ni, Cu, Se, Ag, Cd, Sb, Ba, Pb, and U were determined by ICP-MS. The element Rh, 103 atomic mass unit and 10 μg/L concentration, was used as internal standard in ICP-MS analyses. Elements As and Hg were determined by flow injection online with ICP-MS, hydride and vapor generation, respectively (Cidu, 1996).

For each analytical run, the detection limits (DL) were calculated at 10 times the standard deviation (SD) of the mean value calculated on several analyses of the blank solution, made up of ultrapure water MILLI-Q and supra pure HNO_3 1 % (v/v). It is worth to recall that the dataset for each element used in this study was generated over years. Because the DL may vary depending on instrument performance, different DL values resulted for each element.

In order to check potential contamination during sampling and analysis, blank solutions using MILLI-Q water were prepared in the field (field blank) and processed using the same procedures used for the water samples. Concentrations of trace elements in field blanks were either below or very close to the DL. The standard reference solutions SRM1643d,e (supplied by the US National Institute of Standard & Technology, Gaithersburg, Maryland) and EnviroMAT ES-L-3 (supplied by SCP Science, St. Laurent, Quebec) were used to estimate analytical errors, which varied temporally depending on instrument performances. A few results showing measured concentrations versus certified values of standard reference solutions and the corresponding errors are reported in the Supplementary material (SM Table 1 and SM Table 2). Errors were usually below 10 %; in some cases errors reached a maximum of 14 %.

With reference to the evaluation of groundwater quality, the guidelines established by the WHO (2017) for drinking water and threshold values established by Italian legislations for drinking water and for the protection of groundwater (GURI, 2006; 2009; 2016) were considered. It is worth remembering that the Italian legislation incorporates the European legislation concerning the protection of groundwater against pollution and deterioration (EC, 2006; 2014).

3.3 Statistical analysis

Several data-analysis procedures are available for datasets containing multiple detection limits (Lee and Helsel, 2005). For this study, concentrations below DL were processed as follows: *i)* for dataset containing undetected values below 5 % of samples, the detection limit was substituted with the detection limit itself (elements B, Rb, Sr, Ba, U); *ii)* for dataset containing from 6 % to 75 % of undetected values (elements Li,

Be, Al, V, Cr, Mn, Fe, Co, Ni, Cu, Zn, As, Se, Mo, Cd, Pb), the detection limit was substituted using the Regression on Order Statistics method (ROS method, Shumway et al., 2002; Lee and Helsel, 2005); *iii)* for dataset containing more than 75% of undetected values (elements Ag, Sb, Te, Hg, Tl, Bi) no substitution was made and the undetected values were disregarded. In general, if the information drawn from the variance-covariance matrix structure is sufficiently high, and cases are numerous, the method proposed by Martin-Fernandez et al. (2015) would be preferable. In our case, significant differences by the application of different methods were not observed.

Summary statistics were calculated after the DL substitution (with the exception of elements Ag, Sb, Te, Hg, Tl, Bi having a large number of undetected values) and included the median value, selected percentiles, MAD and IQR. Histogram, cumulative probability plot and boxplot were used as exploratory data tools (Reimann et al., 2008; Filzmoser et al., 2009; Grunsky, 2010; Reimann and de Caritat, 2017; Sahoo et al., 2019).

The bias effect related to the compositional nature of geochemical data was taken into account for elements B, Al, Mn, Fe, Co, Ni, Cu, Zn, As, Cd, Ba, Pb and U (other elements were not considered due to a large number of undetected concentrations) using the centered log-ratio (*clr*) transformation (Aitchison, 1986) where for the composition $\mathbf{x} = (x_1, x_2, \dots, x_D)$ with *D* components or variables is defined as:

$$clr(\mathbf{x}) = \left(log \frac{x_1}{g_m(\mathbf{x})}, log \frac{x_2}{g_m(\mathbf{x})}, \dots, log \frac{x_D}{g_m(\mathbf{x})} \right)$$

where $g_m(\mathbf{x}) = \prod_{i=1}^{D} x_i^{1/D}$ is the geometric mean of the row.

In order to investigate multivariate relationships and potential correlations between chemical elements, the compositional *clr*- biplot was then performed (Daunis-I-Estadella et al., 2006; Pawlowsky-Glahn and Buccianti, 2011; Gozzi et al., 2020).

The threshold values were calculated considering different estimators. For the elements containing less than 75 % of undetected values (Be, B, Al, V, Cr, Mn, Fe, Co, Ni, Cu, Zn, As, Se, Cd, Ba, Pb and U) the threshold values were calculated using: *i)* mean+2SD (Standard Deviation), *ii)* median+2MAD, *iii)* the TIF estimator, and *iv)* selected percentiles of the distribution (95^{th} and 97.7^{th}). Calculations were performed on the log-transformed data, then threshold values were obtained back-transforming the results. It should be noted that percentiles of the distribution are not influenced by the logarithmic transformation. For elements Li, Rb, Sr, Mo, containing less than 75 % of undetected values but with a limited number of samples in the dataset, the threshold values were estimated using the percentiles of the distribution, either 95^{th} or 97.7^{th}. For elements Ag, Te, Tl, Sb, Hg and Bi, having a limited number of samples in the dataset and/or more than 75 % of undetected values, the threshold values were not calculated, but a distribution map was drawn.

Statistical analyses were accomplished with the free language for statistical computing R version 3.6 (R Development Core Team, 2013) and the package NADA (Nondetects And Data Analysis) was used for the ROS method. Also, the free open source CoDaPack software (Comas-Cufí and Thió-Henestrosa, 2011) was used to perform the *clr*- transformation of raw data and the *clr*- biplot.

The groundwater composition given by B, Al, Mn, Fe, Co, Ni, Cu, Zn, Ba and U was used for the searching of the "baseline composition". The robust Mahalanobis distance of each composition from the robust barycenter of a homogeneous group of data was determined following the approach reported in Verboven and Hubert (2005), after to have transformed the data in isometric coordinates (Egozcue et al., 2003). For each geological complex with which the groundwater comes into contact the distance-distance plot was obtained displaying robust distance (RD_i) versus classical Mahalanobis distance (MD_i). The horizontal and vertical lines in the RD_i - MD_i plot are drawn at the cut-off value:

$$\sqrt{\chi^2_{p,0.975}}$$

with *p* number of variables.

Geochemical maps were drawn using ArcGIS 10.2 (ESRI, 2013).

4. Results

4.1 Summary statistics

The summary statistics of concentrations of trace elements is reported in Table 1, together with the drinking water guidelines established by the Italian Government and the WHO. Among the analyzed elements only Sr showed concentrations above DL in all samples. Elements Li, B, Cu, Zn, Rb, Ba and U showed less than 10 % of undetected values; V, Mn and Mo undetected concentrations were in the range of 21 to 49 %; Be, Al, Cr, Fe, Co, Ni, As, Se, Cd and Pb had 56 % to 72 % of undetected values; Ag, Sb, Te, Hg, Tl and Bi showed undetected values ranging from 86 % to 99 % (Table 1).

Among the regulated elements, the concentrations of Cr (maximum value 14 µg/L) and Ba (maximum value 486 µg/L) in the studied waters were always below guidelines (Table 1). The highest value of Cu (1380 µg/L) occurred in groundwater at one single sampling site; excluding that value, the maximum concentration of Cu measured was 116 µg/L, i.e. lower than the Italian and WHO guidelines (1000 and 2000 µg/L, respectively). Elements B, Al, V, Ni, Sb, Tl and U showed values above guidelines in <1.0 % of samples, whereas Mn, Fe, As, Se, Cd, Hg and Pb showed a percentage of values above guidelines in the range of 1.0 (Cd) to 9.2 % (Mn).

4.2 Element associations

The median concentration of Li, Be, B, Al, V, Cr, Mn, Fe, Co, Ni, Cu, Zn, As, Se, Rb, Sr, Cd, Ba, Pb and U, i.e. those elements having undetected values below 75 %, grouped by the geological complex with which groundwater samples come into contact, are reported in Table 2. As compared with regional values, relatively high median concentrations of Zn, Cd, Ba and Pb were observed in groundwater interacting with Paleozoic carbonate rocks (Table 2), likely reflecting the occurrence of relevant Cd-bearing sphalerite [(Zn,Cd)S], barite [$BaSO_4$] and galena [PbS] deposits (Boni et al., 1999), which location is shown in Figure 1. Vanadium and Cr median concentrations were relatively high in groundwater interacting with the Quaternary basalt, indicating a lithological control on their concentration in groundwater, which was in agreement with literature records (Wright and Belitz, 2010).

Based on values reported in Table 2, a compositional *clr*- biplot was drawn in order to identify relevant element associations, which may indicate specific geochemical processes and/or particular geological environments. The resulting compositional biplot is shown in Figure 2, in which the first two components describe about 82 % of the cumulative data set variability, thus indicating the presence of a strong variance-covariance structure.

The longest rays from the origin were for Quaternary basalt and Paleozoic carbonate (Fig. 2). This indicates that the ratio of concentration of these components to all others is responsible for most of the variability across all samples. The shortest ray from the origin was for the Tertiary sediment group, implying that the ratio of concentration of these components to all others was less variable. Different geochemical associations of elements with the geological complexes were observed. In particular, Zn, Cd and Pb were associated with the Paleozoic carbonate group (Fig. 2), confirming the interaction of groundwater with the diffused ore deposits hosted in these rocks in the Iglesiente-Fluminese Zn-Pb mine district (Fig.1). The relative concentration in groundwater and the geochemical associations of elements showed in Figure 2 indicate that the median concentration of each element in groundwater was mostly influenced by the interaction of water with specific lithological compositions and/or by the presence of mineralization, highlighting a relevant role of the geological availability on the concentration of trace elements in groundwater. Interesting in the biplot is also the collinearity between basalt and granitic rock vectors revealing the presence of a subcomposition with a strong one-dimensional variability (Daunis-I-Estadella et al., 2006).

4.2 Regional threshold values

The threshold values calculated using different methods for Li, Be, B, Al, V, Cr, Mn, Fe, Co, Ni, Cu, Zn, As, Se, Rb, Sr, Mo, Cd, Ba, Pb and U in the Sardinian groundwater samples are reported in Table 3, together with guidelines established by the Italian Government and the WHO reported for comparison. The application of different estimators resulted in different threshold values. Threshold values calculated assuming the 95^{th} percentile provided the most conservative estimate. Threshold values calculated by the 97.7^{th} percentile, the Mean+2SD and the Median+2MAD were within the same order of magnitude. The TIF method usually provided the highest threshold values, generally higher than the 97.7^{th} value, except for Mn and Fe that showed many outliers.

For elements Li, Rb, Sr, and Mo the threshold values corresponding to 95^{th} and 97.7^{th} value of distribution, might be assumed as a provisional threshold estimate due to the small number of data available. The regional threshold values of the regulated elements B, Al, V, Cr, Cu and Cd, whatever the method used, were below the Italian and WHO drinking water guidelines. All calculated threshold values for Mn were higher than the

Italian guideline value of 50 µg/L. Although Mn is not suspected of causing direct health effects through its presence in drinking water, high concentrations should be considered because may result in severe discoloration of water, and frequently may cause operational problems (WHO, 2017). The regional threshold values of As were mostly above the Italian and WHO drinking water guidelines. The regional threshold values calculated by TIF for Ni, Se, Pb and U exceeded the respective guidelines (Table 3).

4.3 Explorative maps

Here, the As, Cd and Pb maps are discussed first due to the toxicity of these elements to human health and their relevance in the protection of groundwater against pollution and deterioration. Maps for others elements are provided in the supplementary material (SM Figures 1, 2 and 3) and will be discussed later.

Figure 3 shows the maps of As, Cd and Pb concentrations, with symbol sizes corresponding to the threshold value calculated using different estimators based on the log-transformed data. The highest concentrations were usually associated to areas of known mineralization (see Fig. 1).

High concentrations of As in groundwater (Fig. 3a) were related to the oxidative dissolution of arsenopyrite [FeAsS] and enargite [Cu_3AsS_4] in Tertiary volcanic rocks, respectively in the north (Osilo; Biddau and Cidu, 2005) and central (Furtei; Cidu et al., 2013) Sardinia, and to the diffuse occurrence of arsenopyrite in metamorphic rocks in southeast Sardinia (Fig. 1, Gerrei; Frau et al., 2012).

Elevated Cd concentrations in groundwater samples were mostly observed in south Sardinia (Fig. 3b), mostly related to the interaction of water with sphalerite mineralization. The Pb map (Fig. 3c) showed relatively high concentrations in groundwater draining the Iglesiente-Fluminese mining districts that host relevant galena deposits (Fig. 1).

Figure 4 shows the maps of As, Cd and Pb derived from the *clr*- data. The *clr*- map does not express direct information about the concentration of the investigated element at each point in the land. Instead, it represents a relative abundance of each element with respect to the geometric mean of all elements considered. In addition to the areas highlighted in the As concentration map (Fig. 3a), the *clr*- As map allowed to distinguish other areas with relative As-enrichment, specifically, in northern Sardinia and close to Oristano (Fig. 4a). Small differences were observed when comparing the concentrations map of Cd (Fig. 3b) and Pb (Fig. 3c) with the *clr*- maps of Cd (Fig. 4b) and Pb (Fig. 4c).

The maps for elements Li, Be, V, Cr, Se, Rb, Sr and Mo in Sardinian groundwater are reported in the SM Figure 1, together with the cumulative plot, histogram and boxplot.

Threshold values for Li, Rb, Sr and Mo, determined in a small number of groundwater samples, were calculated using the 95^{th} and 97.7^{th} percentiles. The highest concentrations of Li, Rb and Sr (SM Figures 1a, f, g, respectively) were mainly observed in groundwater interacting with Tertiary andesite and ignimbrite that underwent hydrothermal alteration (Biddau and Cidu, 2005). Concentrations of Mo (SM Figure 1h) above the 97.7^{th} threshold occurred in groundwater draining areas hosting known mineralization (e.g. the Gerrei district shown in Fig. 1; Cidu et al., 2021).

Elements Be, V, Cr and Se were determined in a large number of groundwater samples, thus threshold values were calculated using all estimators. The maps of Be, V, Cr and Se (SM Figures 1b, c, d, e, respectively) showed relatively high concentrations mostly in groundwater draining Tertiary and Quaternary environments in western Sardinia. Few spots with high Be and Cr occurred in groundwater draining granitic rocks (SM Figures 1b, d), probably due to associated pegmatite.

The concentration maps and *clr*- maps for elements B, Al, Mn, Fe, Co, Ni, Cu, Zn, Ba and U, are shown in the SM Figure 2, together with the cumulative plot, histogram and boxplot.

The regional distributions of B showed high concentrations in groundwater interacting with marine-derived sediments of Miocene age (SM Figure 2a). The *clr*- B map also showed groundwater interacting with basalt and andesite to be relatively enriched in B (SM Figure 2b).

High concentrations of Al were mostly observed in volcanic, granitic and metamorphic rocks, i.e. in silicate environments (SM Figure 2c).

Relatively high occurrences of Mn (SM Figure 2e, f), Fe (SM Figure 2g, h), Co (SM Figure 2i, j), Ni (SM Figure 2k, l), Cu (SM Figure 2m, n), Zn (SM Figure 2o, p) and Ba (SM Figure 2q, r) in groundwater appeared unrelated to specific rocks, although high concentrations associated with mineralized areas were recognized (Sinisi et al., 2012). Groundwater samples interacting with Quaternary basalt and Tertiary andesite were relatively enriched in Ba (SM Figure 2r).

Concentrations of U above the WHO guideline were mainly observed in groundwater draining granitic rocks (SM Figure 2s).

Concentration maps for elements Ag, Sb, Te, Hg, Tl, and Bi, showing a high number of undetected values (94, 86, 98, 90, 87 and 99 %, respectively, Table 1), are reported in the SM Figure 3, together with the cumulative curve and box plot. Concentrations of these elements above DL were observed in groundwater draining known mineralized areas. Concentrations of Ag (SM Figure 3a), Sb (SM Figure 3b) and Hg (SM Figure 3d) above DL were only measured in 63, 170 and 108 groundwater samples, respectively, i.e. ≤ 14 % of total samples analyzed. Detected concentrations of these elements corresponded to groundwater draining mineralized areas (Fig. 1), both mined (Iglesiente-Fluminese, Gerrei) and not exploited (Osilo, Tertenia). Concentrations of Hg above the drinking water guideline were also observed in groundwater draining Quaternary sediments in southern Sardinia (SM Figure 3d).
Concentrations of Te, Tl, and Bi above DL occurred in very few groundwater samples located in mineralized areas (SM Figures 3c, e, f, respectively).

5. Discussion

In general, the 95th and the Median+2MAD estimators of each trace element most likely represent the threshold value at the regional scale. Threshold values calculated by other estimators might be more appropriate at the local scale. It is worth mentioning that classical concentration maps are useful for many practical applications and the *clr*- maps can deliver additional information in some, though not all, cases (Reinmann et al., 2012).
Among the regulated elements in drinking water, As, Cd and Pb have high environmental relevance. The regional threshold in Sardinian groundwater may range from 5 to 16 µg/L As, 0.5 to 0.6 µg/L Cd, and 2.5 to 4.3 µg/L Pb (95th and median+2MAD in Table 3). Concentrations of these elements above the regional threshold values mainly occurred in groundwater draining areas of known mineralization, highlighting the relevant role of element abundances in rocks and sediments with which the groundwater interacts. Moreover, most of As, Cd and Pb are hosted in sulfide minerals that can be easily dissolved when they come in contact with water and oxygen. Schematic reactions of [FeAsS], [Cu_3AsS_4], [(Zn,Cd)S] and [PbS] dissolution are showed in equations 1, 2, 3 and 4, respectively (Plumlee, 1999; Dold, 2010; Cidu et al., 2018):

$$4FeAsS + 13O_2 + 6H_2O \rightarrow 4Fe^{2+} + 4H_2AsO_4^- + 4SO_4^{2-} + 4H^+ \quad (1)$$

$$Cu_3AsS_4 + 8.75O_2 + 2.5H_2O \rightarrow 3Cu^{2+} + AsO_4^{3-} + 4SO_4^{2-} + 5H^+ \quad (2)$$

$$(Zn_{(1-x)}Cd_x)S + 2O_2 \rightarrow (1-x)Zn^{2+} + xCd^{2+} + SO_4^{2-} \quad (3)$$

$$PbS + 2O_2 \rightarrow Pb^{2+} + SO_4^{2-} \quad (4)$$

The *clr*- As map allowed to identify relatively high concentrations of As also in areas where mineral deposits are not documented. In particular, in northern Sardinia a relative enrichment of As in groundwater was associated with Tertiary andesite and ignimbrite (Fig. 4a) that may host disseminate As-bearing sulfide minerals (Simeone et al., 2005). Another As cluster was observed close to Oristano in the Quaternary sediment group (Fig. 4a). In this flat area alluvia and lacustrine sediments are often rich in organic matter that may promote reductive dissolution of Fe(III) and Mn(IV) hydroxides/oxides according with schematic reactions 5 and 6, which in turn would also release sorbed As into solution (Frau et al., 2019).

$$CH_2O + 4Fe(OH)_3 + 7H^+ \rightarrow 4Fe^{2+} + HCO_3^- + 10H_2O \quad (5)$$

$$CH_2O + 2MnO_2 + 3H^+ \rightarrow 2Mn^{2+} + HCO_3^- + 2H_2O \quad (6)$$

This interpretation would be in agreement with a relative enrichment of Mn observed in the same area (SM Figure 2e, f).
The *clr*- Cd (Fig. 4b) and Pb (Fig. 4c) maps were similar to those drawn using concentration values, probably due to the prevalent association of these elements with widespread mineralization of Zn(Cd) and Pb in Sardinia, which is in agreement with literature results (Cidu et al., 2009).
A small cluster with relatively high Pb was observed in the northwest Sardinia (Fig. 4c) in groundwater circulating in Mesozoic carbonate. In such environment, the formation of aqueous complexes such as $PbCO_3^0$ is favored, which in turn would allow Pb to remain in groundwater due to the stability of this

complex (Stumm and Morgan, 1996) under the near-neutral to slightly alkaline pH in groundwater of this area observed in this study and in literature (Da Pelo et al., 2017).

The regulated elements Sb, Hg and Tl showed a high number of undetected values. Notwithstanding this critical aspect, regional threshold values might range from 1.1 to 2.0 µg/L Sb, from 0.6 to 0.9 µg/L Hg, and from 0.4 to 0.5 µg/L Tl (95^{th} and 97.7^{th} in Table 1). Antimony concentrations above the regional threshold occurred in areas of known mineralization (e.g. Osilo, Iglesiente-Fluminese, Gerrei; see Fig. 1 for location). Concentrations above the Italian drinking water limit of 5 µg/L Sb were observed in 0.7 % of total samples (Table 1). Mercury concentrations above the drinking water limit of 1 µg/L (1.6 % of total samples, Table 1) occurred in areas of known mineralization (SM Figure 3d). Indeed, in the Iglesiente-Fluminese mining district Hg was enough abundant to be recovered as byproduct from galena ore (Cidu et al, 2001). High concentrations of Hg were also found in groundwater in the Campidano Plain and nearby urban areas. Such concentrations were apparently unrelated with geogenic processes. Therefore, these areas should be investigated in more detail to pinpoint eventual anthropogenic contamination. Concentrations of Tl were below 0.7 µg/L in 99 % of total samples. The three samples with Tl concentrations slightly above the Italian guideline occurred in groundwater located nearby the mineralized area of Osilo and in granitic rocks of southern Sardinia (SM Figure 3e). In this case, more sampling sites would be required to assess the regional occurrence of Tl above the guideline of 2 µg/L. Being a regulated element, we suggest that the determination of Tl should be included in the groundwater monitoring programs established by the Regional and National Governments.

Elements B, Al, V, Cr, Mn, Fe, Ni, Cu, Se, Ba and U are also regulated in drinking water. Groundwater samples with relatively high concentrations of B were mainly associated with marine-derived sediments and with volcanic rocks. These findings appear consistent with relatively high B in seawater, and in volcanic rocks that underwent hydrothermal alteration (Ryan and Langmuir, 1993). Relatively high concentrations of Al were mostly observed in volcanic, granitic and metamorphic rocks, i.e. in silicate environments where Al is a major component. About 1 % of total groundwater samples had Al concentrations above guidelines, sometimes associated with low pH, which is consistent with increasing solubility of Al at pH < 6 (Stumm and Morgan, 1996). High concentrations of Al might be also associated with particles < 0.4 µm in size, to which Al would be sorbed.

Elements V and Cr (SM Figures 1c, d, respectively) showed relatively high concentrations mostly in groundwater draining Quaternary basalt, Tertiary andesite and ignimbrite in northwest Sardinia, which was in agreement with relatively high V and Cr contents reported in these rocks (Lustrino et al., 2013).

Elements Mn, Fe, Ni and Cu in groundwater often occurred in areas of known mineralization. Concentrations of Mn and Fe above guidelines were observed in 9.2 % and 4 % of total samples, respectively (Table 1). Relatively high Mn and Fe occurrences were associated with different geological complexes (SM Figure 3e, f), which appeared to be consistent with the diffused Mn and Fe abundance in crustal rocks (Rudnick and Gao, 2014). As compared to aqueous Fe, the ion Mn^{2+} is stable under a wide pH and redox range in natural waters (Stumm and Morgan, 1996), which may account for the widespread high concentrations of Mn in the Sardinian groundwater. These observations, also considering that a Mn guideline was not established by WHO, pose a question on the Italian guideline of 50 µg/L Mn, a concentration probably inadequate for representing natural conditions, and establishing the *good* status of groundwater.

Concentrations of Se above guidelines were observed in 1.8 % of total samples (Table 1), mostly associated with groundwater draining Quaternary and Tertiary sediments (SM Figure 1e), for which the Se abundance is unknown.

Relatively high concentrations of Ba occurred in groundwater interacting with kaolin deposits (SM Figure 2r), which would be consistent with literature records (Dill et al., 1995). High concentrations of Ba sometimes occurred in groundwater having low sulfate (not shown), highlighting the role of barite equilibrium in controlling aqueous Ba concentrations.

The highest concentrations of U were observed in groundwater draining granitic environments (SM Figure 2s, t), as expected considering the U content in granite higher than mafic rocks, and the U mobility as ion uranyl (UO_2^{2+}) and its complexes under oxic conditions (Campbell et al., 2015).

Elements Li, Be, Co, Zn, Rb, Sr, Mo are not regulated in drinking water. Variations in concentrations were found dependent on the interaction of water with specific rocks (Li, Be, Rb, Sr usually enhanced in Tertiary formations; Mormone and Piochi, 2020) and/or with mineral deposits (Co, Zn, Mo; see Fig. 1).

In summary, different estimators were used to calculate regional threshold values of trace elements in groundwater. The most conservative estimate at the regional scale was the assumption of the 95^{th} percentile. Other estimators usually provided higher threshold values that should be considered at the local scale.

Elements Mn, Fe, Ni, As, Se, Pb and U in groundwater showed threshold values, calculated by one or more estimators, above guidelines established for drinking water. The geochemical characteristics of groundwater and regional distribution maps showed that high concentrations and outliers values of these elements were mostly associated to groundwater interacting with rocks enriched in specific elements and/or with mineral deposits. In addition to the geogenic abundance of trace elements, physical-chemical parameters and geochemical characteristics may contribute in enhancing concentrations in groundwater, e.g. via reductive dissolution driven by organic matter (As), the formation of stable aqueous complexes (Pb), equilibrium with respect to solid phases (Ba), without neglecting the role of colloidal/ very fine particles as potential sorption sites for elements such as Al, Mn, Fe and As.

Both maps, i.e. concentration and *clr*-, are needed to understand the processes governing the spatial distribution of trace elements in groundwater. The use of *clr*- maps, compared with the classical ones, permitted to constrain the element source, giving a more complete picture of the behavior of each element with respect to the other components in groundwater. In particular, the *clr*- maps were useful to pinpoint critical areas to be investigated in more detail. In such areas, groundwater sampling and analyses should be implemented for understanding ongoing processes and pinpoint potential sources of groundwater contamination. In these conditions the *clr*- data spatial distribution might reveal, in fact, decoupling phenomena of some elements respect to the expected geochemical behavior, thus revealing unknown inputs or perturbations.

The interesting results obtained with the *clr*- maps allowed us to further improve, under CoDA principles, the searching of the *baseline composition*, thus abandoning single elements and considering the fundamental links of the chemical species in the composition to which they pertain. The composition given by B, Al, Mn, Fe, Co, Ni, Cu, Zn, Ba and U was used for this purpose. An example is reported in Figure 5 for groundwater interacting with the Paleozoic metamorphic rocks. Data located in the upper right quadrant were related to outliers or extreme compositions, whereas those located toward the down left corner were near to the robust barycenter. In the case of groundwater interacting with metamorphic rocks the most extreme compositions were given by groundwater samples located downstream of known mineralization, which is consistent with high concentrations of trace elements due to the interaction of groundwater with the ore deposits. The composition closer to the robust barycenter in Figure 5 was given by the spring sample N45 that was located far away either from mineralization or anthropogenic activities, thus close to nearly pristine environmental conditions.

The application of the analysis to the different geological complexes has allowed to identify the composition of groundwater samples closer to the compositional barycenter. These samples are listed in Table 4, with locations shown in the SM Figure 4. The Robust Mahalanobis distance (RD_i) threshold value separating anomalous or extreme compositions from the rest of the data for each geological complex is also reported in Table 4. The RD_i threshold values correspond to the horizontal red line in the distance-distance plots drawn for groundwater interacting with the different geological complexes, reported in the Supplementary Material (SM Figure 5).

The composition of the groundwater samples listed in Table 4, characterized by joint relationships among B, Al, Mn, Fe, Co, Ni, Cu, Zn, Ba and U, could be considered as a reference in groundwater monitoring plans at different scales. In fact, these compositions might represent the *baseline condition* of groundwater interacting with a specific geological complex, and the answer to perturbation of the reference groundwater sample might give interesting early warning signals about environmental changes.

6. Conclusions

Establishing the actual natural quantification of aqueous components is mandatory to identify significant and feasible clean-up goals (European Water Framework Directive 2000/60/EC, article 17). The application of remediation strategies, simply following compliance levels established by current regulations, might lead to ineffective and unaffordable targets at sites where specific natural conditions may cause geogenic contamination of water systems. Following the assessment of contamination status with respect to baseline conditions at contaminated sites, remediation actions might be better planned by National and Regional Governments.

Results of this study indicate the need of excluding those samples surely affected by anthropogenic activity when assessing baseline conditions in groundwater, i.e. an accurate pre-selection should be carried out before data processing. To this purpose hydrogeochemical interpretations of data was a valuable tool in highlighting interactions of water with solid and gas phases, better predicting relations among elements, and recognize anthropogenic effects. Also, selecting the reliable variables to be used on data processing was mandatory. In

this framework, the methodology proposed under CoDA able to recognize extreme or outlier compositions with respect to those closer to the compositional barycenter can give a substantial contribution to recognize processes at the base of anomalous behavior of trace elements, as well as more representative, perhaps pristine/stable, conditions.

The methodology adopted in this study appears adequate to distinguish effective anthropogenic contamination from natural conditions. Therefore, results of this study may help stakeholders to define realistic environmental clean-up goals, and consequently planning adequate strategies to reduce groundwater contamination at specific areas. The peculiarity of Sardinia where varied mineral occurrences are widespread in the island (Marcello et al., 2008) should be also considered. Indeed, a common feature among the considered trace elements was that concentrations in groundwater increased depending on the geological availability in rocks hosting the water bodies. In addition to the geological abundance, specific conditions may play a significant role in enhancing the geochemical mobilization and spatial distribution of trace elements.

As reported in the recent 2022 IPCC report (https://www.ipcc.ch/report/ar6/wg2/) climate change is causing substantial damages and increasingly irreversible losses in terrestrial freshwater at different scales, so that any investigation of the baseline of a Country represents a fundamental starting point to evaluate and quantify resilience of ecosystems and human communities.

Acknowledgements

Research funded by the Regione Autonoma della Sardegna (Cooperation Agreement between DSCG-UNICA and RAS-ADIS-STGRI, CIG Z552D570E8, scientific responsible R. Cidu).

References

Aitchison, J., 1986. The Statistical Analysis of Compositional Data. pp 416, Chapman & Hall, London.

Allègre, C. J., Lewin, E., 1995. Scaling laws and geochemical distributions. Earth and Planetary Science Letters 132, 1– 13.

Appelo, C.A.J., Postma D., 1993. Geochemistry, groundwater and pollution. 2nd Edition, pp 536, A.A. Balkema, Rotterdam.

Biddau, R., Cidu, R., 2005. Hydrogeochemical baseline studies prior to gold mining: A case study in Sardinia (Italy). Journal of Geochemical Exploration 86, 61–85.

Biddau, R., Cidu, R., Lorrai, M., Mulas M.G., 2017. Assessing background values of chloride, sulfate and fluoride in groundwater: A geochemical-statistical approach at a regional scale. Journal of Geochemical Exploration 181, 243–255.

Binda, G., Pozzi, A., Livio, F., Piasini, P., Zhang, C., 2018. Anomalously high concentration of Ni as sulphide phase in sediment and in water of a mountain catchment with serpentinite bedrock. Journal of Geochemical Exploration 190, 58–68.

Birke, M., Reimann, C., Oorts, K., Rauch, U., Demetriades, A., Dinelli, E., Ladenberger, A., Halamic, J., Gosar, M., Jähne-Klingberg, F., G.E.M.A.S. Project Team. 2016. Use of GEMAS data for risk assessment of cadmium in European agricultural and grazing land soil under the REACH regulation. Science of the Total Environment 74, 109–121.

Boente, C., Albuquerque, M.T.D., Gallego, J.,R., Pawlowsky-Glahn, V., Egozcue, J.J., 2022. Compositional baseline assessments to adress soil pollution. An application in Langreso, Spain. Science of the Total Environment 812, 15383.

Boni, M., Costabile, S., De Vivo, B., Gasparrini, M., 1999. Potential environmental hazard in the mining district of southern Iglesiente (SW Sardinia, Italy). Journal of Geochemical Exploration 67, 417–430

Buccianti, A., Grunsky, E., 2014. Compositional data analysis in geochemistry: are we sure to see what really occurs during natural processes. Journal of Geochemical Exploration 141, 1–5.

Campbell, K.M., Gallegos, T.J., Landa, E.R., 2015. Biogeochemical aspects of uranium mineralization, mining, milling, and remediation. Applied Geochemistry 57, 206–235.

Carmignani, L., Oggiano, G., Funedda, A., Conti, P., Pasci, S., 2015. The geological map of Sardinia (Italy) at 1:250,000 scale. Journal of Maps 12, 826–835.

Cidu, R., 1996. Inductively coupled plasma - mass spectrometry and - optical emission spectrometry determination of trace elements in water. Atomic Spectroscopy 17, 155–162.

Cidu, R., Biagini, C., Fanfani, L., La Ruffa, G., Marras, I., 2001. Mine closure at Monteponi (Italy): effect of the cessation of dewatering on the quality of shallow groundwater. Applied Geochemistry 16, 489–502

Cidu, R., Biddau, R., Fanfani, L., 2009. Impact of past mining activity on the quality of groundwater in SW Sardinia (Italy). Journal of Geochemical Exploration 100, 125–132.
Cidu, R., Biddau, R., Frau, F., Wanty, R.B., Naitza, S., 2021. Regional occurrence of aqueous tungsten and relations with antimony, arsenic and molybdenum concentrations (Sardinia, Italy). Journal of Geochemical Exploration 229, 106846
Cidu, R., Da Pelo, S., Frau, F., 2013. Legacy of cyanide and ARD at a low-scale gold mine (Furtei, Italy). Mine Water and the Environment 32, 74–83.
Cidu, R., Dore, E., Biddau, R., Nordstrom, D.K., 2018. Fate of antimony and arsenic in contaminated waters at the abandoned Su Suergiu mine (Sardinia, Italy). Mine Water and the Environment 37,151–165.
Comas-Cufí, M., Thió-Henestrosa S., 2011. CoDaPack 2.0: a stand-alone, multi-platform compositional software. In: Egozcue JJ, Tolosana-Delgado R, Ortego MI, eds. CoDaWork'11: 4th International Workshop on Compositional Data Analysis. Sant Feliu de Guíxols.
Da Pelo, S., Ghiglieri, G., Buttau, C., Biddau, R., Cuzzocrea, C., Funedda, A., Carletti, A., Vacca, S., Cidu, R., 2017. Coupling 3D hydrogeological modelling and geochemical mapping for an innovative approach to support management of aquifers. Italian Journal of Engineering Geology and Environment, Special Issue 1, DOI: 10.4408/IJEGE.2017-01.S-04
Daunis-I-Estadella, J., Barcelo-Vidal, C., Buccianti, A., 2006. Exploratory compositional data analysis. In: Compositional Data Analysis in the Geosciences: from theroy to practice, Buccianti, A., Materu-Figueras, G. and Pawlowsky-Glahn, V. (eds). Geological Society, London, Special Publications 264, 161–174.
De Vivo, B., Boni, M., Costabile, S., 1998. Baseline formational anomalies versus mining pollution: geochemical risk maps of Sardinia, Italy. Journal of Geochemical Exploration 64, 321–337.
Dill, H.G., Fricke, A., Henning, K.-H., 1995. The origin of Ba- and REE-bearing aluminium-phosphate-sulphate minerals from the Lohrheim kaolinitic clay deposit (Rheinisches Schiefergebirge, Germany). Applied Clay Science 10, 231–245.
Dold, B., 2010. Basic Concepts in Environmental Geochemistry of Sulfidic Mine-Waste Management. Waste Management, Er Sunil Kumar (Ed.), ISBN: 978-953-7619-84-8.
EC (European Community), 2006. Council Directive 2006/118/EC, on the protection of groundwater against pollution and deterioration. Off. J. European Commission, Bruxelles.
EC (European Community), 2014. Commission Directive 2014/80/EU of 20 June 2014 amending Annex II to Directive 2006/118/EC of the European Parliament and of the Council on the protection of groundwater against pollution and deterioration. Off. J. European Commission, Bruxelles.
Edmunds, W.M., Shand, P., Hart, P., Ward, R.S., 2003. The natural (baseline) quality of groundwater: a UK pilot study. Science of the Total Environment 310, 25–35.
Egozcue, J.J., Pawlowsky-Glahn, V., Mateu-Figueras, G., Barcelo-Vidal, C., 2003. Isometric Logratio Trasformations for Compositional Data Analysis. Mathematical Geology, 35(1), 280–300.
ESRI, 2013. Environmental Systems Research Institute, Esri, 380 New York Street, Redlands, California 92373-8100, USA.
Filzmoser, P., Hron, K., Reimann, C., 2009. Principal component analysis for compositional data with outliers. Environmetrics 20, 621–632.
Funedda, A., Naitza, S., Buttau, C., Cocco, F., Dini, A., 2018. Structural Controls of Ore Mineralization in a Polydeformed Basement: Field Examples from the Variscan Baccu Locci Shear Zone (SE Sardinia, Italy). Minerals 8, 456; doi:10.3390/min8100456.
Frau, F., Cidu, R., Ardau, C., 2012. Short-term changes in water chemistry in the Baccu Locci stream (Sardinia, Italy) affected by past mining. Applied Geochemistry 27(9), 1844–1853.
Frau, F., Cidu, R., Casu, M., Soriga, A., 2019. Assessing arsenic sources in landfill areas: a case study in Sardinia. Italian J. Geosciences 138, 116–123, https://doi.org/10.3301/IJG.2018.30
Gozzi, C., Sauro Graziano R., Buccianti A., 2020. Part-whole relations: new insights about the dynamics of complex geochemical riverine systems. Minerals, 10(6), 501.
Grunsky, E.C., 2010. The interpretation of geochemical survey data. Geochemistry Exploration Environment Analysis 10, 27–74.
GURI (Gazzetta Ufficiale della Repubblica Italiana), 2006. Decreto legislativo 3 aprile 2006, n. 152 Norme in materia ambientale. Gazzetta Ufficiale della Repubblica Italiana n. 88 del 14-4-2006, suppl. ord. n. 96, Roma (in Italian).
GURI (Gazzetta Ufficiale della Repubblica Italiana), 2009. Decreto legislativo 16 marzo 2009, n. 30. Attuazione della direttiva 2006/118/CE, relativa alla protezione delle acque sotterranee dall'inquinamento e dal deterioramento. Gazzetta Ufficiale della Repubblica Italiana n. 79 del 4-4-2009, Roma (in Italian).

GURI (Gazzetta Ufficiale della Repubblica Italiana), 2016. Decreto legislativo 6 luglio 2016. Recepimento della direttiva 2014/80/UE della Commissione del 20 giugno 2014 che modifica l'allegato II della direttiva 2006/118/CE del Parlamento europeo e del Consiglio sulla protezione delle acque sotterranee dall'inquinamento e dal deterioramento. Gazzetta Ufficiale della Repubblica Italiana n. 165 del 16-7-2016, Roma (in Italian).

IMH (Italian Ministry of Health), 2016. Acque potabili. Tallio. Ministero della Salute - Direzione generale della prevenzione sanitaria. www.salute.gov.it (in Italian).

ISPRA (Istituto Superiore per la Protezione e la Ricerca Ambientale), 2018. Linea guida per la determinazione dei valori di fondo per i suoli e per le acque sotterranee. SNPA, 08 2018, Roma (in Italian).

ISTAT (Istituto Nazionale di Statistica), 2011. Censimento della popolazione 2011. http://www.istat.it/it/sardegna (Last accessed in July 2021).

Kierczak, J., Pietranik, A., Pędziwiatr, A., 2021. Ultramafic geoecosystems as a natural source of Ni, Cr, and Co to the environment: A review. Science of the Total Environment 755, 142620

Langmuir, D., 1997. Aqueous Environmental Geochemistry. Prentice-Hall, 600 p.

Lee, L., Helsel, D., 2005. Baseline models of trace elements in major aquifers of the United States. Applied Geochemistry 20, 1560–1570.

Lohan, M.C., Tagliabue, A., 2018. Oceanic Micronutrients: Trace Metals that are Essential for Marine Life. Elements 14, 385–390, DOI: 10.2138/gselements.14.6.385

Lorrai, M., Mereu, I., 1999. Indagine geochimica sulle acque della zona costiera di Tertenia (Sardegna Orientale). Rendiconti Seminario Facoltà Scienze Università di Cagliari 69, 125–137 (in Italian).

Lustrino, M., Fedele, L., Melluso, L., Morra, V., Ronga, F., Geldmacher, J., Duggen, S., Agostini, S., Cucciniello, C., Franciosi, L., Meisel, T., 2013. Origin and evolution of Cenozoic magmatism of Sardinia (Italy). A combined isotopic (Sr–Nd–Pb–O–Hf–Os) and petrological view. Lithos 180–181, 138–158.

Mameli, P., Mongelli, G., Oggiano, G., Dinelli, E., 2007. Mineralogy and geochemistry of the Nurra bauxites (Western Sardinia): constraints for the conditions of the formation and parental affinity. International Journal Earth Science 96, 887–902.

Marcello, A., Mazzella, A., Naitza, S., Pretti, S., Tocco, S., Valera, P. Valera, R., 2008. Carta metallogenica e delle georisorse della Sardegna, scala 1: 250,000. Litografia artistica e cartografica S.r.l., Firenze (in Italian).

Martin-Fernandez, J.A., Hron, K., Templ, M., Filzmoser, P., Palarea-Albaladejo, J., 2015. Bayesian-multiplicative treatment of count zeros in compositional data sets. Statistical Modelling 15 (2): 134–158.

Matschullat, J., Ottenstein, R., Reimann, C., 2000. Geochemical background - can we calculate it? Environmental Geology 39, 990–1000.

Mongelli, G., Mameli, P., Sinisi, R., Buccione, R., Oggiano, G. 2021. Rees and other critical raw materials in Cretaceous Mediterranean-type bauxite: The case of the Sardinian ore (Italy). Ore Geology Reviews 139, 1-15

Mormone, A., Piochi, M., 2020. Mineralogy, Geochemistry and Genesis of Zeolites in Cenozoic Pyroclastic Flows from the Asuni Area (Central Sardinia, Italy). Minerals 10, 268.

Moroni, M., Naitza, S., Ruggieri, G., Aquino, A., Costagliola, P. De Giudici, G., Caruso, S., Ferrari, E., Fiorentini, M.L., Lattanzi P., 2019. The Pb-Zn-Ag vein system at Montevecchio-Ingurtosu, southwestern Sardinia, Italy: A summary of previous knowledge and new mineralogical, fluid inclusion, and isotopic data. Ore Geology Reviews 115, 103194

Naitza, S., Conte, A.M., Cuccuru, S., Oggiano, G., Secchi, F., Tecce, F., 2017. A Late Variscan tin province associated to the ilmenite-series granites of the Sardinian Batholith (Italy): The Sn and Mo mineralisation around the Monte Linas ferroan granite. Ore Geology Reviews 80, 1259–1278.

Oorts, K., Schoeters, I., 2014. Use of monitoring data for risk assessment of metals in soil under the European REACH regulation. C. Reimann, M. Birke, A. Demetriades, P. Filzmoser, P. O'Connor (Eds.), Chemistry of Europe's Agricultural Soils – Part B: General Background Information and Further Analysis of the GEMAS Data Set, Geologisches Jahrbuch (Reihe B103), Schweizerbarth, Hannover (2014), pp. 189-202.

Palomba, M., Padalino, G., Marchi, M., 2006. Industrial mineral occurrences associated with Cenozoic volcanic rocks of Sardinia (Italy): Geological, mineralogical, geochemical features and genetic implications. Ore Geology Reviews 29, 118– 145.

Parrone, D., Ghergo, S., Preziosi, E., 2019. A multi-method approach for the assessment of natural background levels in groundwater. Science of the Total Environment 659, 884–894.

Parviainen, A., Loukola-Ruskeeniemi, K., 2019. Environmental impact of mineralised black shales. Earth-Science Reviews 192, 65–90.
Pawlowsky-Glahn, V., Buccianti, A., 2011. Compositional data analysis: theory and applications. John Wiley & Sons.
Plumlee, G.S., 1999. The environmental geology of mineral deposits. In: Plumlee, G.S., Logsdon, M.J. (Eds.), The Environmental Geochemistry of Mineral Deposits, Part A. Society of Economic Geologists, Littleton, CO, pp. 71–116.
RAS, 2005. Deliberazione della Giunta Regionale n. 1/12 del 18/01/2005 con cui la Regione Sardegna ha designato, quale zona vulnerabile da nitrati di origine agricola (ZVN), una porzione del territorio del Comune di Arborea. Regione Autonoma della Sardegna, Cagliari (in Italian).
RAS, 2011. Caratterizzazione, obiettivi e monitoraggio dei corpi idrici sotterranei della Sardegna approvato con Deliberazione della Giunta Regionale n. 1/16 del 14/01/2011. Regione Autonoma della Sardegna Cagliari, https://www.regione.sardegna.it/documenti/1_328_20130906131252.zip (in Italian, last accessed in August 2021).
RAS, 2013. Carta geologica di base della Sardegna. Regione Autonoma della Sardegna, Cagliari. http://www.sardegnageoportale.it/argomenti/cartageologica.html (Last accessed in October 2021).
R Development Core Team, 2013. R: A Language and Environment for Statistical Computing. R Foundation for Statistical Computing, Vienna, Austria. http://www.Rproject.org/.
Reimann, C., Birke, M., Demetriades, A., Filzmoser, P., O'Connor, P., 2014a. Chemistry of Europe's Agricultural Soils - Part A: Methodology and Interpretation of the GEMAS Data Set, Geologisches Jahrbuch (Reihe B 102), pp 528, Schweizerbarth, Hannover.
Reimann, C., Birke, M., Demetriades, A., Filzmoser, P., O'Connor, P., 2014b. Chemistry of Europe's Agricultural Soils - Part B: General Background Information and Further Analysis of the GEMAS Data Set, Geologisches Jahrbuch (Reihe B 103), pp 352, Schweizerbarth, Hannover.
Reimann, C., de Caritat, P., 2017. Establishing background variation and threshold values for 59 elements in Australian surface soil. Science of the Total Environment 578, 633–648.
Reimann, C., Fabian, K., Birke, M., Filzmoser, P., Demetriades, A., Negrel, P., Oorts, K., Matschullat, J., de Caritat, P., The GEMAS Project Team., 2018. GEMAS: Establishing geochemical background and threshold for 53chemical elements in European agricultural soil. Applied Geochemistry 88, 302–318.
Reimann, C., Filzmoser, P., Garrett, R.G., Dutter, R., 2008. Statistical Data Analysis Explained: Applied Environmental Statistics with R. John Wiley & Sons, Ltd. ISBN: 978-0-470-98581-6, pp. 362
Reimann, C., Garrett, R.G., Filzmoser, P., 2005. Background and threshold - critical comparison of methods of determination. Science of the Total Environment 346, 1–16.
Rudnick, R.L., Gao, S., 2014. Composition of the Continental Crust. Treatise on Geochemistry 2nd Edition, http://dx.doi.org/10.1016/B978-0-08-095975-7.00301-6
Ryan, J.G., Langmuir, C.H., 1993. The systematics of boron abundances in young volcanic rocks. Geochimica et Cosmochimica Acta 57, 1489–1498
Sahoo, P.K., Dall'Agnol, R., Salomão, G.N., da Silva Ferreira Junior, J., et al., 2019. High resolution hydrogeochemical survey and estimation of baseline concentrations of trace elements in surface water of the Itacaiúnas River Basin, southeastern Amazonia: Implication for environmental studies. Journal of Geochemical Exploration 205, 106321
Simeone, R., Dilles, J.H., Padalino, G., Palomba, M., 2005. Mineralogical and stable isotope studies of kaolin deposits: shallow epithermal systems of western Sardinia, Italy. Economic Geology 100, 115–130.
Sinisi, R., Mameli, P., Mongelli, G., Oggiano, G., 2012. Different Mn-ores in a continental arc setting: Geochemical and mineralogical evidences from Tertiary deposits of Sardinia (Italy). Ore Geology Reviews 47, 110–125
Shumway, R.H., Azari, R.S., Kayhanian, M., 2002. Statistical approaches to estimating mean water quality concentrations with detection limits. Environmental Science Technology 36, 3346-3353.
Smith, D.B., Cannon, W.F., Woodruff, L.G., Ellefsen, K.J., 2014. Geochemical and Mineralogical Maps for Soils of the Conterminous United States. pp 386, United States Geological Survey Open-File Report 2014-1082.
Stumm, W., Morgan, J.J., 1996. Aquatic chemistry, chemical equilibria and rates in natural waters. Third Edition, John Wiley & Sons Inc., New York.
Verboven, S., Hubert, M., 2005. LIBRA: A MATLAB library for robust analysis. Chemometrics and Intelligent Laboratory Systems 75, 127-136.

WHO, 2017. Guidelines for drinking-water quality: fourth edition incorporating the first addendum. World Health Organization, Geneva, ISBN 978-92-4-154995-0.
Wright, M.T., Belitz, K., 2010. Factors controlling the regional distribution of vanadium in groundwater. Ground Water 48, 515–525.
Zanotti, C., Caschetto, M., Bonomi, T., Parini, M., Cipriano, G., Fumagalli, L., Rotiroti, M., 2022. Linking local natural background levels in groundwater to their generating hydrogeochemical processes in Quaternary alluvial aquifers. Science of the Total Environment 805, 150259.
Zoback, M.L., 2001. Grand Challenges in Earth and Environmental Sciences - Science, Stewardship, and Service for the Twenty-First Century. Geological Society of America Today 11 (12), 41–47.

784 Captions
785
786 Figure 1. Location of the study area and simplified lithological map of Sardinia (modified after RAS, 2013) showing
787 main industrial sites, mining districts, mineralized areas (De Vivo et al., 1998; Marcello et al., 2008) and relevant
788 industrial mineral deposits (Palomba et al., 2006).

789 Figure 2. Compositional *clr*- biplot showing the relationship among the median values of selected trace elements in
790 groundwater samples grouped by the geological complexes. The principal component analysis was carried out on data
791 reported in Table 2.

792 Figure 3. Maps of As (a), Cd (b) and Pb (c) in Sardinian groundwater showing threshold values calculated with different
793 methods based on the log-transformed data. The cumulative probability plot, histogram and boxplot are also reported
794 for each element. Red symbols in the maps and cumulative plots indicate concentrations above guidelines.

795 Figure 4. Maps of As (a), Cd (b) and Pb (c) in Sardinian groundwater showing ranges of values calculated on the *clr*-
796 transformed data. Symbol sizes in the maps increase as relative concentrations of each element with respect to all other
797 components in groundwater increase. The cumulative probability plot, histogram and boxplot are also reported for each
798 element.

799 Figure 5. Robust Mahalanobis distance versus classical distance for groundwater samples interacting with metamorphic
800 rocks for the multivariate dataset given by B, Al, Mn, Fe, Co, Ni, Cu, Zn, Ba and U.

801

802 Table 1. Summary statistics of trace elements in Sardinian groundwater and guidelines for drinking water and the
803 protection of groundwater from contamination. DL = detection limit. Min = minimum value. Max = maximum value.
804 MAD = median absolute deviation. IQR = inter quartile range. n = number of samples. nc = not calculated due to a
805 small number of detected values. ne = not established.

806 Table 2. Median concentrations (in µg/L) of trace elements in Sardinian groundwater at regional level and in
807 groundwater grouped by geological complexes. nc = not calculated due to a small number of samples.

808 Table 3. Threshold values (in µg/L) calculated using different estimators on the back transformed log-data. Drinking
809 water guidelines are reported for comparison. MAD = median absolute deviation. SD = standard deviation. nc = not
810 calculated due to a small number of samples. ne = not established. Values above the lower guideline are reported in
811 bold.

812 Table 4. Robust Mahalanobis distance (RD_i values) from the compositional barycenter of the dataset given by B, Al,
813 Mn, Fe, Co, Ni, Cu, Zn, Ba and U, with groundwater samples listed for geological complexes ranked by age. The
814 column on the right reports the RD_i threshold values separating oultiers or extreme compositions.

815

816 Supplementary material. SM Table 1. Concentrations of elements determined by ICP-OES (ARL 3520) and ICP-MS
817 (PerkinElmer ELAN5000) in the standard solution SRM1643d. SD = standard deviation; Δ % = percent difference
818 between the measured value and the certificate value in the standard solution.

819 Supplementary material. SM Table 2. Concentrations of elements determined ICP-MS (PerkinElmer ELAN DRC-e) in
820 the certified solutions SRM1643e and EnviroMat EP-L-3. SD = standard deviation; Δ % = percent difference between
821 the measured value and the certificate value in the standard solution; nr = not reported.

822 Supplementary material. SM Figure 1. Maps for elements Li (a), Be (b), V (c), Cr (d), Se (e), Rb (f), Sr (g) and Mo (h)
823 in Sardinian groundwater, cumulative plot, histogram and boxplot. Threshold values were calculated using different
824 estimators based on log-transformed data. n = number of samples considered in calculations. Concentrations above
825 guidelines are shown with red symbols.

826 Supplementary material. SM Figure 2. Maps for the elements B (a), Al (c), Mn (e), Fe (g), Co (i), Ni (k), Cu (m), Zn
827 (o), Ba (q) and U (s) in Sardinian groundwater, cumulative plot, histogram and boxplot. Threshold values were
828 calculated using different estimators based on log-transformed data. n = number of samples considered in calculations.
829 Concentrations above guidelines are shown with red symbols. The maps of B (b), Al (d), Mn (f), Fe (h), Co (j), Ni (l),
830 Cu (n), Zn (p), Ba (r) and U (t) show ranges of values calculated on the *clr*- data, with symbol sizes increasing as the
831 relative concentration of each element with respect to all other components in groundwater increases.

832 Supplementary material. SM Figure 3. Maps showing raw concentrations (µg/L) of Ag (a), Sb (b), Te (c), Hg (d), Tl (e)
833 and Bi (f) in Sardinian groundwater, together with the cumulative plot of total samples and the box plot of samples
834 having concentrations above DL. The threshold values for these elements were not calculated due to a high number of
835 undetected values. Classes of symbols in the Ag, Sb, Hg and Tl maps are based on the corresponding boxplot. n =
836 number of samples considered. Concentrations of Sb, Hg and Tl above guidelines are shown with red symbols.

Supplementary material. SM Figure 4. Simplified lithological map of Sardinia showing the location of groundwater samples listed in Table 4.

Supplementary material. SM Figure 5. Robust Mahalanobis distance versus classical distance for groundwater samples interacting with different geological complexes for the multivariate dataset given by B, Al, Mn, Fe, Co, Ni, Cu, Zn, Ba and U.

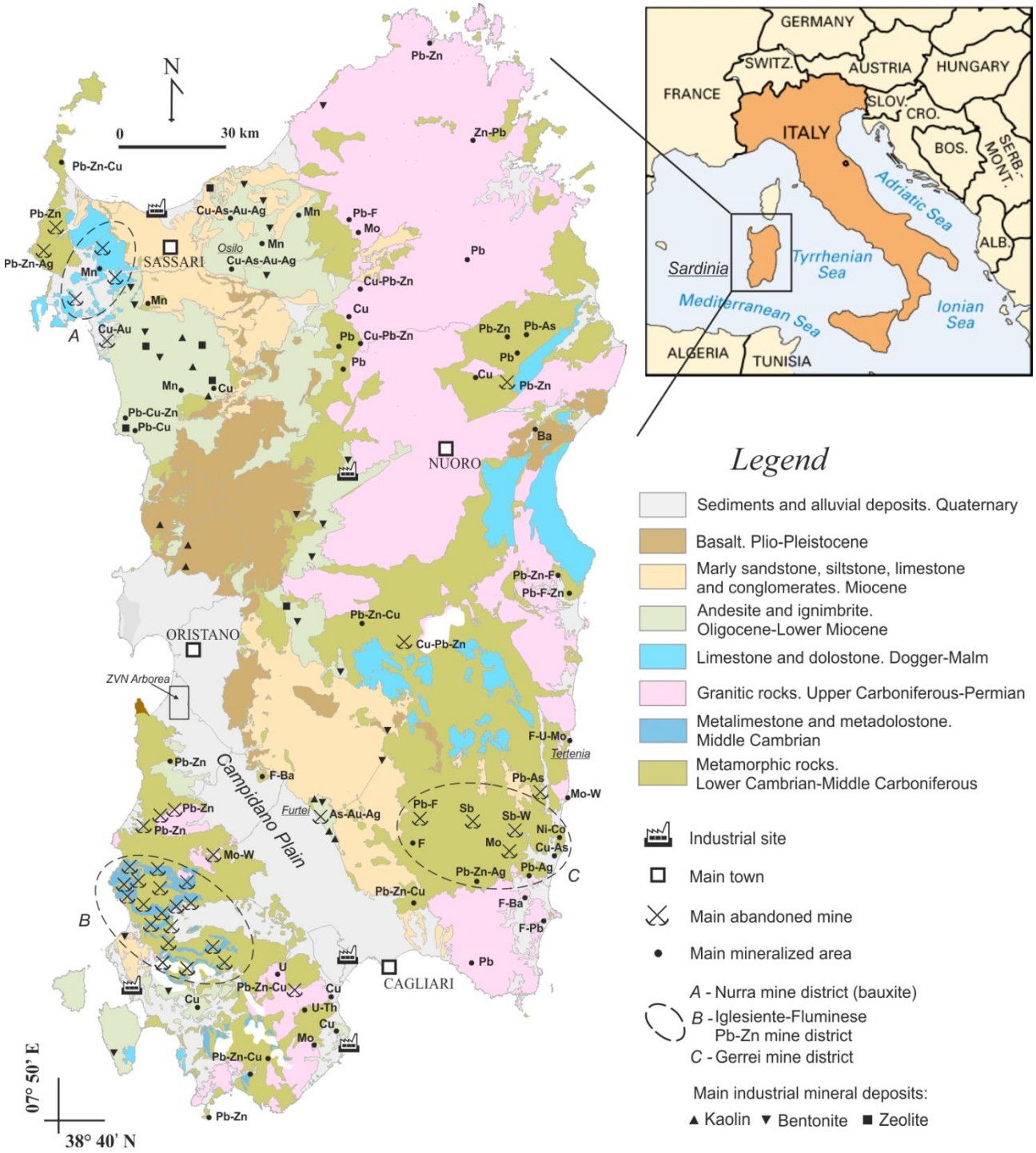

Figure 1. Location of the study area and simplified lithological map of Sardinia (modified after RAS, 2013) showing main industrial sites, mining districts, mineralized areas (De Vivo et al., 1998; Marcello et al., 2008) and relevant industrial mineral deposits (Palomba et al., 2006).

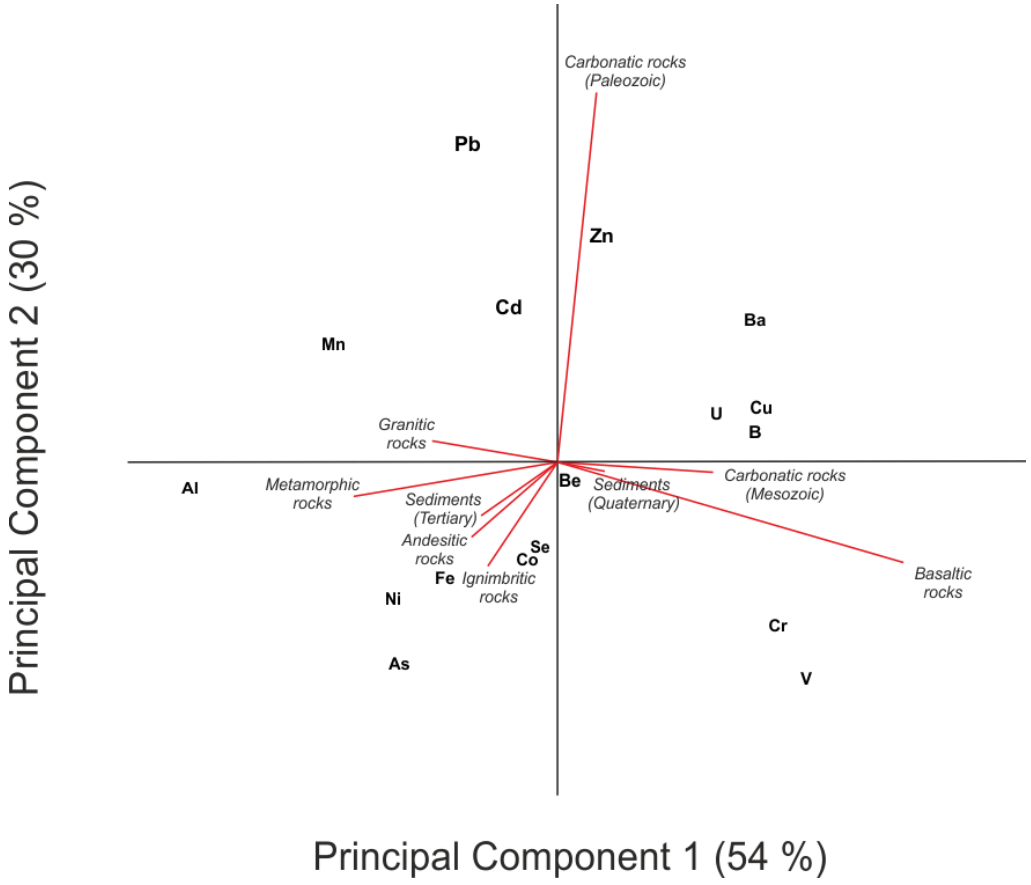

Figure 2. Compositional *clr*- biplot showing the relationship among the median values of selected trace elements in groundwater samples grouped by the geological complexes. The principal component analysis was carried out on data reported in Table 2.

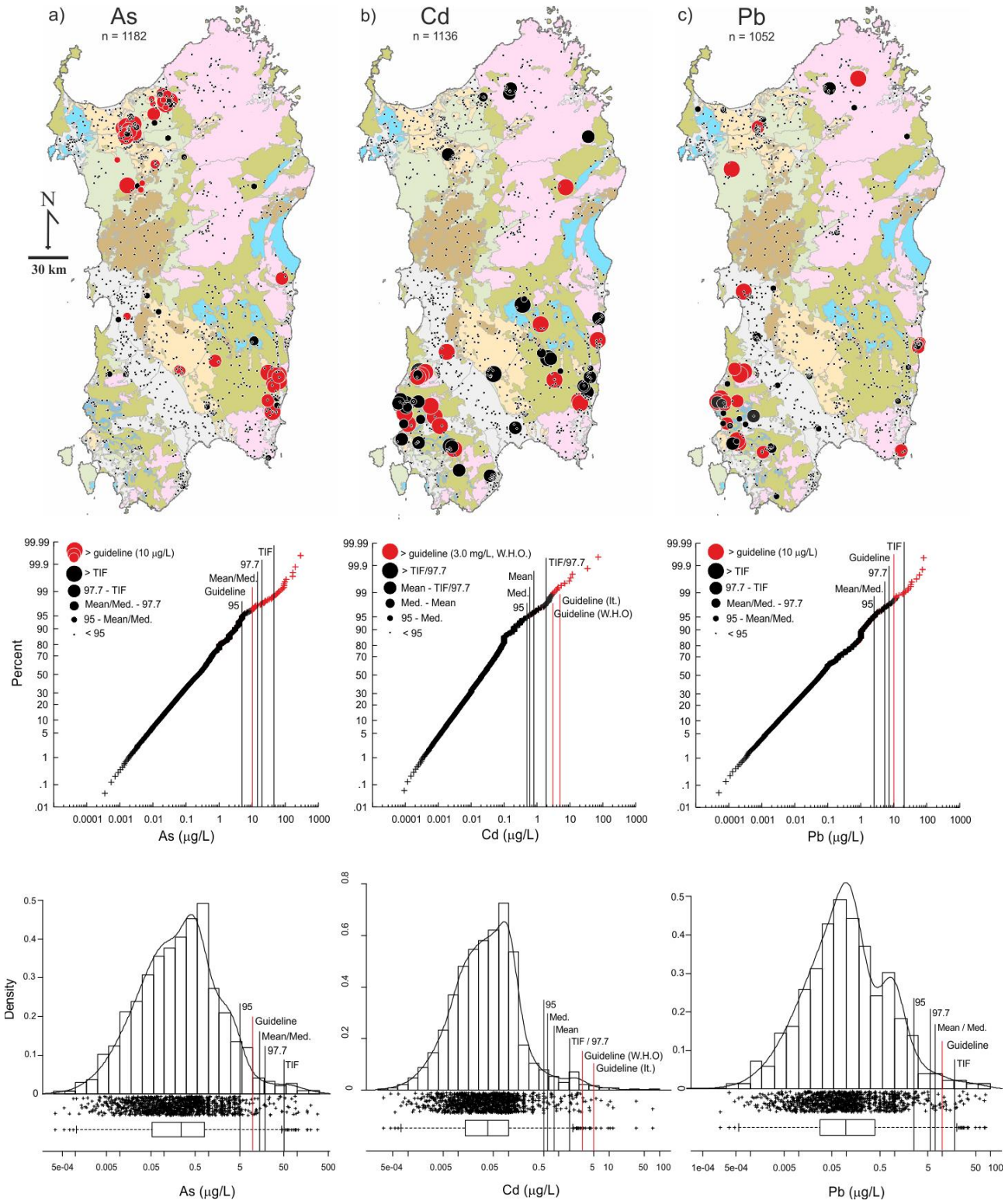

Figure 3. Maps of As (a), Cd (b) and Pb (c) in Sardinian groundwater showing threshold values calculated with different methods based on the log-transformed data. The cumulative probability plot, histogram and boxplot are also reported for each element. Red symbols in the maps and cumulative plots indicate concentrations above guidelines.

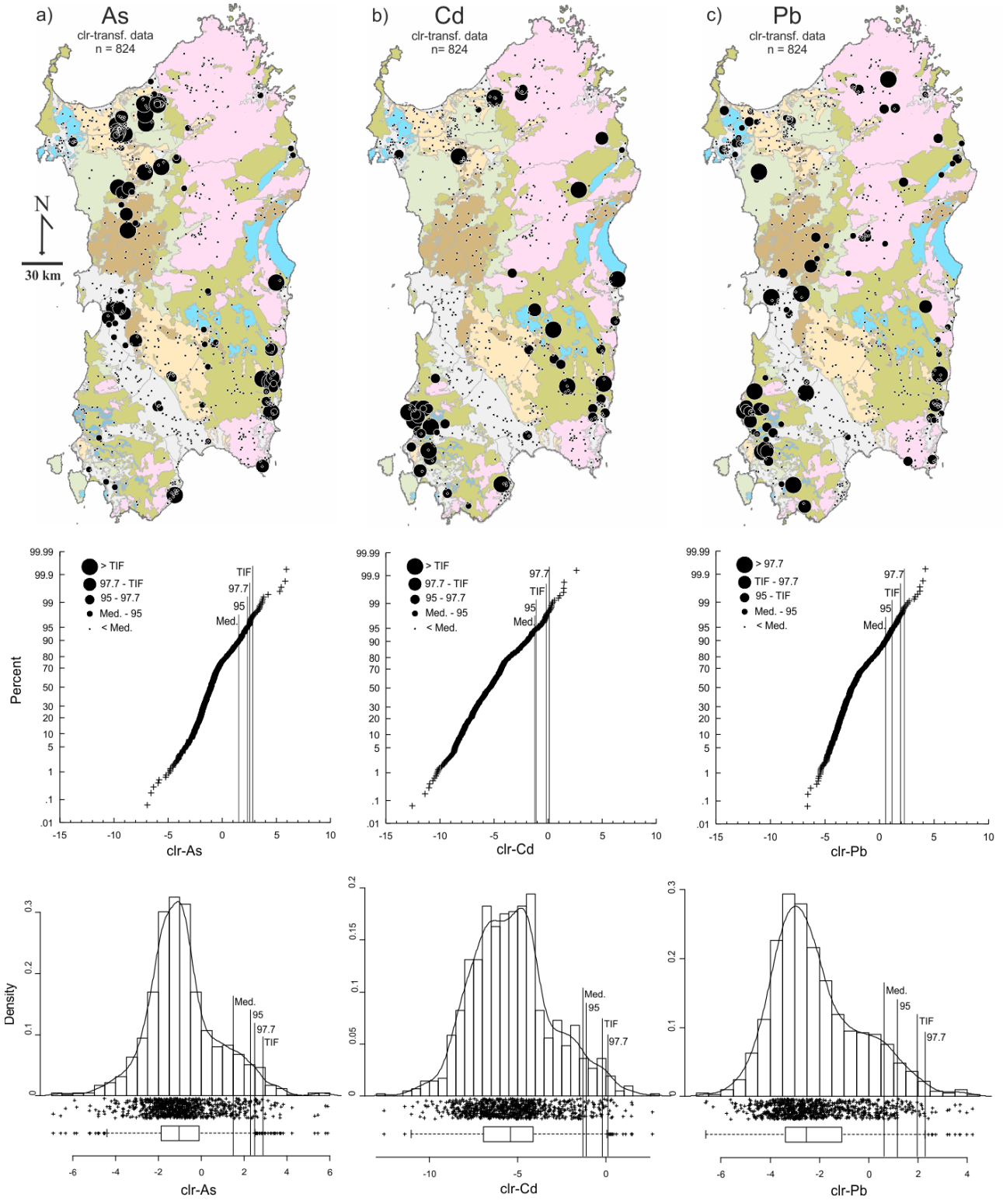

Figure 4. Maps of As (a), Cd (b) and Pb (c) in Sardinian groundwater showing ranges of values calculated on the *clr*-transformed data. Symbol sizes in the maps increase as relative concentrations of each element with respect to all other components in groundwater increase. The cumulative probability plot, histogram and boxplot are also reported for each element.

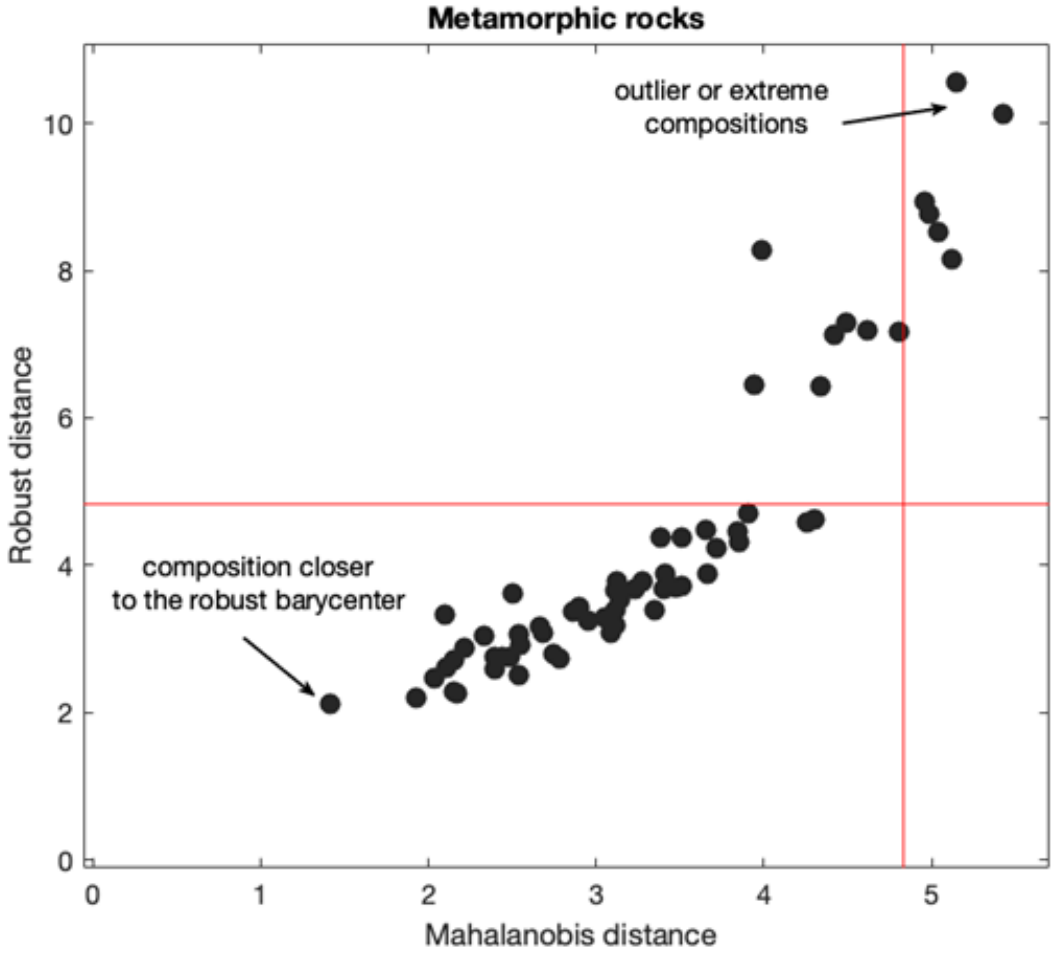

Figure 5. Robust Mahalanobis distance versus classical distance for groundwater samples interacting with metamorphic rocks for the multivariate dataset given by B, Al, Mn, Fe, Co, Ni, Cu, Zn, Ba and U.

Table 1. Summary statistics of trace elements in Sardinian groundwater and guidelines for drinking water and the protection of groundwater from contamination. DL = detection limit. Min = minimum value. Max = maximum value. MAD = median absolute deviation. IQR = inter quartile range. n = number of samples. nc = not calculated due to a small number of detected values. ne = not established.

Element	total	>DL	<DL	<DL	Min	Max	MAD	IQR	25th	Median	75th	80th	90th	95th	97.7th	99th	Guidelines µg/L		% above guideline [c]
	n	n	n	%	µg/L	µg/L	µg/L	µg/L	µg/L	µg/L	µg/L	µg/L	µg/L	µg/L	µg/L	µg/L	Italian [a]	WHO [b]	
Li	356	332	24	7	<5	840	7.2	15	3.4	7.4	18	21	38	78	150	301	ne	ne	nc
Be	1149	506	643	56	<0.01	2.1	0.07	0.2	0.03	0.07	0.20	0.20	0.40	0.60	0.91	1.5	ne	ne	nc
B	1227	1212	15	1	<8	1700	44	73	27	51	100	119	184	302	470	921	1000	2400	0.9
Al	1159	391	768	66	<0.01	5600	0.15	0.8	0.03	0.11	0.84	1.4	8.1	19	62	180	200	ne	0.9
V	984	776	208	21	<0.04	71	0.89	2.0	0.50	1.0	2.5	3.3	6.5	10	15	31	50	ne	0.3
Cr	1009	383	626	62	<0.2	14	0.30	0.9	0.13	0.28	1.0	1.0	2.0	2.3	3.7	5.0	50	50	0
Mn	1212	615	597	49	<0.5	4000	0.88	4.4	0.29	1.0	4.7	7.0	31	150	470	1492	50	ne	9.2
Fe	1200	393	807	67	<3	22,000	1.7	11	2.3	6.7	14	17	40	122	640	2949	200	ne	4.0
Co	1216	425	791	65	<0.01	59	0.04	0.09	0.03	0.06	0.11	0.13	0.30	0.71	3.0	8.1	ne	ne	nc
Ni	1174	465	709	60	<0.07	56	0.25	0.9	0.07	0.20	0.93	1.0	2.0	3.7	6.3	12	20	70	0.4
Cu	1152	1042	110	10	<0.2	1380	1.3	2.4	0.55	1.1	3.0	3.6	7.0	15	23	34	1000	2000	0
Zn	1029	966	63	6	<1.0	3200	12	23	2.5	9.2	25	33	76	191	420	772	ne	ne	nc
As	1182	396	786	66	<0.1	288	0.32	0.7	0.05	0.24	0.80	1.0	3.0	5.0	20	62	10	10	3.4
Se	1027	287	740	72	<0.5	89	0.62	1.8	0.20	0.54	2.0	2.0	3.0	4.7	7.8	16	10	40	1.8
Rb	339	333	6	2	<0.1	183	1.2	4.1	0.41	1.0	4.5	6.8	14	23	32	52	ne	ne	nc
Sr	376	376	0	0	20	14,000	123	197	73	150	270	315	653	1288	2000	3528	ne	ne	nc
Mo	320	198	122	38	<0.01	76	0.24	0.5	0.09	0.20	0.59	0.84	2.0	7.7	16	29	ne	ne	nc
Ag	1099	63	1036	94	<0.01	1.3	nc	nc	<0.04	<0.04	<0.04	<0.05	<0.1	0.12	0.27	1.0	ne	ne	nc
Cd	1136	262	874	72	<0.01	73	0.004	0.09	0.01	0.04	0.10	0.11	0.20	0.50	1.8	3.1	5	3	1.0
Sb	1173	170	1003	86	<0.04	24	nc	nc	<0.2	<0.2	<0.2	<0.3	0.60	1.1	2.0	2.3	5	20	0.7
Te	192	3	189	98	<0.03	0.5	nc	nc	<0.03	<0.06	<0.1	<0.4	<0.4	<0.5	<0.5	0.5	ne	ne	nc
Ba	1215	1191	24	2	<1.0	486	30	49	12	29	61	68	98	136	170	210	ne	1300	0
Hg	1037	108	929	90	<0.1	4.5	nc	nc	<0.1	<0.1	<0.1	<0.2	0.40	0.60	0.90	1.8	1	6	1.6
Tl	323	41	282	87	<0.01	5.9	nc	nc	<0.04	<0.05	<0.1	<0.2	0.35	0.40	0.50	0.78	2 [d]	ne	0.9
Pb	1052	406	646	61	<0.04	80	0.08	0.4	0.028	0.10	0.39	0.60	1.1	2.5	7.1	19	10	10	1.8
Bi	280	3	277	99	<0.01	16	nc	nc	<0.04	<0.1	<0.3	<0.3	<0.6	<1.0	<1.0	2.0	ne	ne	nc
U	1171	1123	48	4	<0.01	151	1.0	1.9	0.22	0.77	2.1	2.6	5.7	11	19	29	ne	30 [e]	0.9

a - GURI, 2006; 2009; 2016. b - WHO, 2017. c - Lower guideline value was considered. d - Provisional guideline value IMH, 2016. e - Provisional guideline value WHO, 2017.

Table 2. Median concentrations (in µg/L) of trace elements in Sardinian groundwater at regional level and in groundwater grouped by geological complexes. nc = not calculated due to a small number of samples.

		Quaternary		Tertiary			Mesozoic	Paleozoic		
Element	Regional	Sediment	Basalt	Sediment	Andesite	Ignimbrite	Carbonate	Granite	Metamorphic	Carbonate
Li	7.4	nc	0.20	30	12	3.4	1.4	7.1	6.9	6.6
Be	0.07	0.10	0.006	0.10	0.06	0.049	0.015	0.05	0.06	0.02
B	50	82	32	74	58	44	38	25	21	48
Al	0.11	0.07	0.002	0.70	0.33	0.38	0.010	1.3	3.6	0.05
V	1.0	1.3	3.7	1.0	2.9	2.0	0.6	0.7	0.6	0.10
Cr	0.28	0.20	0.73	0.40	0.36	0.28	0.05	0.12	0.20	0.034
Mn	1.0	0.4	0.013	1.4	4.0	0.8	0.06	2.0	3.0	1.0
Fe	6.7	4.0	0.3	13	12	8.1	0.9	11	10	0.55
Co	0.06	0.04	0.005	0.11	0.10	0.07	0.012	0.020	0.09	0.008
Ni	0.20	0.10	0.008	0.3	0.9	0.18	0.025	0.34	0.9	0.02
Cu	1.1	2.0	1.0	1.0	1.0	1.0	1.0	0.7	1.0	1.5
Zn	9.2	8.9	1.6	7.0	11	8.6	3.6	9.9	21	50
As	0.24	0.15	0.005	0.6	0.3	1.8	0.022	0.04	0.6	0.011
Se	0.5	0.4	0.04	1.1	0.60	0.65	0.11	0.2	0.6	0.07
Rb	1.0	nc	1.9	10	7.6	3.8	0.5	0.4	0.8	1.8
Sr	150	nc	177	611	334	137	64	105	136	105
Mo	0.2	nc	0.30	1.1	0.20	0.30	0.14	0.2	0.3	0.06
Cd	0.04	0.029	0.002	0.09	0.051	0.061	0.006	0.012	0.1	0.11
Ba	29	49	19	30	18	16	16	12	18	73
Pb	0.10	0.04	0.003	0.15	0.12	0.080	0.009	0.16	0.11	1.0
U	0.8	1.0	0.3	1.4	0.4	0.8	0.7	0.9	0.2	0.7

Table 3. Threshold values (in µg/L) calculated using different estimators on back transformed log-data. Drinking water guidelines are reported for comparison. MAD = median absolute deviation. SD = standard deviation. TIF = Tukey Inner Fence. nc = not calculated due to a small number of samples. ne = not established. Values above the lower guideline are reported in bold.

	Back transformed ln-data					Guidelines	
Element	95th	Median+2MAD	97.7th	Mean+2SD	TIF	Italian [a]	WHO [b]
Li	78	nc	150	nc	nc	ne	ne
Be	0.6	1.3	0.9	1.0	4.0	ne	ne
B	302	366	470	435	719	1000	2400
Al	19	13	62	35	126	200	ne
V	10	11	15	16	28	50	ne
Cr	2.3	6.1	3.7	4.2	23	50	50
Mn	**150**	**61**	**470**	**181**	**302**	50	ne
Fe	122	87	**640**	200	192	200	ne
Co	0.7	1.0	3.0	1.1	2.0	ne	ne
Ni	3.7	9.3	6.3	7.2	**48**	20	70
Cu	15	11	23	20	37	1000	2000
Zn	191	282	420	350	814	ne	ne
As	5.0	**16**	**20**	**15**	**46**	10	10
Se	4.7	10	7.8	10	**62**	10	40
Rb	23	nc	32	nc	nc	ne	ne
Sr	1288	nc	2000	nc	nc	ne	ne
Mo	7.7	nc	16	nc	nc	ne	ne
Cd	0.5	0.6	1.8	0.8	1.9	5	3
Ba	136	313	170	245	691	ne	1300
Pb	2.5	4.3	7.1	5.3	**21**	10	10
U	11	20	19	24	**62**	ne	30

a = GURI, 2006; 2009; 2016. b = WHO, 2017.

Table 4. Robust Mahalanobis distance (RD_i values) from the compositional barycenter of the dataset given by B, Al, Mn, Fe, Co, Ni, Cu, Zn, Ba and U, with groundwater samples listed for geological complexes ranked by age. The column on the right reports the RD_i threshold values separating oultiers or extreme compositions.

Sample	**Geological complex**	***RD*$_i$ values**	***RD*$_i$ threshold values**
13101PO0028 - well	Quaternary sediment	1.85	4.9
17104PO0004 - well		1.84	
22101SO0001 - spring	Quaternary basalt	1.31	5.1
23101PO0059 – well	Tertiary sediment	1.51	5.1
27203PO0004 - well	Tertiary ignimbrite	1.82	4.2
31101PO0006 - well	Tertiary andesite	1.98	4.85
34101SO0005 - spring	Mesozoic carbonate	1.29	8.2
N13 - spring	Paleozoic Granite	1.83	4.9
N17 - spring		1.92	
BG1 - well	Paleozoic carbonate	1.33	4.9
37101PO0003 - well		1.59	
N45 - spring	Metamorphic rocks	1.92	4.7